RSC Advances

This is an *Accepted Manuscript*, which has been through the Royal Society of Chemistry peer review process and has been accepted for publication.

Accepted Manuscripts are published online shortly after acceptance, before technical editing, formatting and proof reading. Using this free service, authors can make their results available to the community, in citable form, before we publish the edited article. This *Accepted Manuscript* will be replaced by the edited, formatted and paginated article as soon as this is available.

You can find more information about *Accepted Manuscripts* in the Information for Authors.

Please note that technical editing may introduce minor changes to the text and/or graphics, which may alter content. The journal's standard Terms & Conditions and the Ethical guidelines still apply. In no event shall the Royal Society of Chemistry be held responsible for any errors or omissions in this *Accepted Manuscript* or any consequences arising from the use of any information it contains.

ROYAL SOCIETY OF CHEMISTRY

www.rsc.org/advances

The phase evolution, electrical stability and chemical compatibility of sealing glass-ceramics for Solid Oxide Fuel Cell Applications: Effect of La_2O_3 or CeO_2

Honglin Liu[1], Xinhang Du[1], Zhiwu Yu[2], Dian Tang[1], and Teng Zhang[1,*]

[1]College of Materials Science and Engineering, Fuzhou University, Fuzhou, Fujian, 350108, China.

[2]High Magnetic Field Laboratory, Hefei Institutes of Physical Science, Chinese Academy of Sciences, Hefei 230031, Anhui, China

Abstract

In spite that rare earth oxides can improve the sealing property of glass-ceramics, the electrical stability of these glass-ceramics under Solid Oxide Fuel Cell (SOFC) operational conditions still remains ambiguous. In this work, the electrical stability of glass-ceramics doped with La_2O_3 or CeO_2 under SOFC operational conditions has been systematically investigated. The glass-ceramic with La_2O_3 dopant exhibits good electrical stability under SOFC operational conditions; whereas, the decrease in the conductivity of the CeO_2-containing glass-ceramic can be related to the formation of a conductive phase, *i.e.*, CeO_2. In particular, the relationship between the phase evolution and the change in conductivity of glass-ceramics has been clearly demonstrated. Moreover, the sealing glass-ceramics show good chemical compatibility with 8 mol% yttria-stabilized zirconia (8YSZ) electrolyte, after held at 750 ºC for 1000 hours. The reported results support the suitability of La_2O_3-containing glass-ceramic as sealing material for SOFC application.

Key words: solid oxide fuel cell, glass-ceramics, electrical stability, chemical compatibility

* Corresponding author 1: Tel.: +86 591 22866540; fax: +86 591 22866537.
Email address: teng_zhang@fzu.edu.cn (T. Zhang).

RSC Advances Accepted Manuscript

1. Introduction

The direct operation of Solid Oxide Fuel Cell (SOFC) on hydrocarbon fuels has attracted increasing attention in the last decade, due to the large amount of hydrocarbons as well as the highest conversion efficiency of SOFC among all types of fuel cells. Planar SOFC have become increasingly attractive, due to its lower cost and higher power density per unit volume compared with tubular designs.[1-5] However, there are many edges that need to be sealed at high temperature. Therefore, sealing materials are of great importance for the planar SOFC components. Sealing glasses and glass-ceramics have been proved to be the most promising candidates, and thus constitutes a very active filed of research.[6-10]

To accomplish the sealing target of planar SOFC, many requirements on sealing materials need to be fulfilled, including sealing properties, thermal stability, thermo-mechanical stability, electrical stability, as well as chemical compatibility.[11-14] To reduce the coefficient of thermal expansion (CTE) mismatch between sealing glass-ceramics and other SOFC components, network modifiers, *e.g.*, alkaline earth metal oxides[15,16] and alkaline metal oxides,[17,18] are often included in the sealing materials. However, the presences of such mobile ions contributes to the increase in electrical conductivity of glasses and glass-ceramics,[19,20] and thus, imposes additional uncertainty on the electrical insulation of sealing glass-ceramics, especially under long-term operation of SOFC. For example, Huang *et al.*[21] reported a Y_2O_3–BaO–SiO_2–B_2O_3–Al_2O_3 glass sealant with a CTE of 11.64 K^{-1} between 323 and 873 K, which falls in the desired CTE range for SOFC applications (9-12×10^{-6} K^{-1}).[16,22] However, its conductivity is about 5×10^{-6} S·cm^{-1} at 750 ºC, mainly due to the high BaO content in glass (60 wt%). In addition, the conductivity of a

RSC Advances Accepted Manuscript

SrO-La_2O_3-Al_2O_3-B_2O_3-SiO_2 glass developed by Ojha *et al*. ranges from 2.70×10^{-6} to 5.68×10^{-7} $S\cdot cm^{-1}$ in the temperature range of 600-800 ºC.[23] Therefore, the electrical property of sealing glass-ceramics attracts increasing attentions in recent years.[6,24-27]

On the other hand, rare earth oxides such as La_2O_3 and CeO_2 have been proved to be beneficial for the sintering property of glass-ceramics,[22,28] which is highly desired for SOFC sealing application. However, the effect of rare earth oxides on the electrical stability of glass-ceramics under SOFC operational conditions still remains ambiguous, which needs to be clarified before they could be seriously considered as sealing candidates for SOFC applications.

In this paper, La_2O_3 or CeO_2 was added into a representative borosilicate glass system, respectively. Attention was focused on the effect of La_2O_3 or CeO_2 on the electrical stability of glass-ceramics under SOFC operational conditions. In particular, the relationship between the phase evolution and the change in conductivity of glass-ceramics was established to provide useful information for the development of reliable sealing materials for SOFC applications.

2. Experimental

A 50-g sample of glass designated ‘GA’ was prepared from a batch mixture of reagent grade alkaline earth carbonates, boric acid, and various oxides to form the nominal glass composition (mol%): $25.0CaO$-$25.0SrO$-$10.0Al_2O_3$-$7B_2O_3$-$33.0SiO_2$. The glasses doped with La_2O_3 or CeO_2 were also prepared with the nominal glass compositions (mol%) of $24.5CaO$-$24.5SrO$-$9.8Al_2O_3$-$6.9B_2O_3$-$32.3SiO_2$-$2La_2O_3$ and $24.0CaO$-$24.0SrO$-$9.6Al_2O_3$-$6.7B_2O_3$-$31.7SiO_2$-$4CeO_2$, respectively. The sealing glasses with La_2O_3 or CeO_2 dopant are designated as glass#GL and glass#GC, respectively. The mole fractions of La or Ce ions in glasses are designed to be 4 mol% for comparison. The batches were melted in a platinum crucible at a temperature of

RSC Advances Accepted Manuscript

1400-1500°C for 2 hours in air. Some of the melt was poured into stainless steel mold to obtain cylindrical shaped glass specimens (25 mm length and 10 mm diameter) and the rest of the melt was quenched on a steel plate. Glass powders were then crushed and sieved to a particle size of 45 to 53 μm.

Pellets (10 mm diameter and 2 mm thickness) were formed by uniaxial pressing of the glass powders before heating at 750 °C for up to 1000 h. A high resistance meter (4339B, Agilent, Inc.) was used to measure the conductivity of the glasses and glass-ceramic pellets in air from 600 to 750 ºC.

The coefficient of thermal expansion (CTE, between 200 and 600 ºC), glass transition temperature (T_g) and softening temperature (T_d) of quenched glasses were determined by dilatometer (DIL402C, NETZSCH, Inc.) at 10 ºC·min^{-1} in air. The glass-ceramic samples held at 750 ºC for 1000 hours were also subjected to CTE measurement for comparison. Thermal properties of glasses and glass-ceramics, including T_g, T_d and CTE, are summarized in Table 1.

The crystalline phases in the glass-ceramic samples were identified by X-ray diffraction (XRD, XDS 2000, Scintag, Inc.). The relative content of crystalline phases (in wt%) in CeO_2-containing species was then calculated by RIQAS software (Release 4.0.0.8, Materials Data, Inc., CA).

The glass-ceramic pellets were polished using SiC paper from 320 to 1200 grit, and then finished using an alumina suspension (3 μm). The polished samples were analyzed using field emission scanning electron microscopy (Supra-55, Zeiss, Inc.) and energy dispersive analysis by X-rays (X-Max, OXFORD instruments, Inc.). The glasses were bonded to an 8 mol% YSZ (8YSZ) electrolyte (AR, Sinopharm Chemical Reagent Co., Ltd., China) and their interfacial reactions were characterized. Glass pastes were prepared by mixing ~50 mg of the glass powder (particle size of

RSC Advances Accepted Manuscript

45-53 μm) with ~50 μL of acetone. The pastes were applied to the 8YSZ surfaces after ultrasonic cleaning. The coated were subsequently heated in air at 750 ºC for 1000 h. Cross sections of the glass/8YSZ sealing couples were polished and analyzed using FE-SEM and EDS.

3. Results and discussion

Fig.1a shows the conductivity of glasses measured in air from 600 to 750 ºC. It is clear that the conductivity of glasses increases with increasing temperature. This denotes that the ionic conduction is the main mechanism in present work.[29,30] In addition, the conductivity of glasses decreases with addition of La_2O_3 or CeO_2. For example, the conductivity of glasses at 750 ºC decreases from 8.05×10^{-7} S·cm^{-1} for glass#GA to 2.63×10^{-7} S·cm^{-1} for glass#GC and to 1.90×10^{-7} S·cm^{-1} for glass#GL. It is worth noting that the conductivity of La_2O_3-containing glass-ceramics is about two order of magnitude lower than that of the SrO-La_2O_3-Al_2O_3-B_2O_3-SiO_2 glass under similar condition (*e.g.*, 1.03×10^{-8} vs. 2.70×10^{-6} S·cm^{-1}, measured at 600 ºC).[23] The Arrhenius plots in Fig. 1a has been fitted to calculate the activation energy of ionic conduction in glass. The similar activation energy, ranging from 145±10 to 160±10 kJ mol^{-1}, confirms the same conductive mechanism in all glasses.

Fig.1b shows the conductivity of glass-ceramics held at 750 ºC for 1000 h. The conductivity of glass-ceramics increases with increasing temperature, exhibiting the characteristic of ionic conduction. It is clear that the conductivity of glass#GA and glass#GL is much lower than that of glass#GC. In addition, the activation energy of ionic conduction in glass-ceramics increases from 124±10 kJ mol^{-1} for glass#GC to 150±10 kJ mol^{-1} for glass#GA.

To investigate the electrical stability of glass-ceramics under SOFC operational environment, the conductivity of glass-ceramics measured at 750 ºC is plotted as a

RSC Advances Accepted Manuscript

function of heat-treatment time, as shown in Fig.1c. The conductivity of glass#GA and glass#GL decreases slightly with increasing time and reaches a constant after 500 h; whereas, the conductivity of glass#GC increases by an order of magnitude in the first 100 h, and then decreases to a constant after 500 h. For example, the conductivity of glass#GL after held at 750 ºC for 24, 100, 500, and 1000 h is 1.00×10^{-7}, 6.70×10^{-8}, 3.38×10^{-8}, and 4.16×10^{-8} $S\cdot cm^{-1}$, respectively. In contrast, the conductivity of glass#GC after held at 750 for 24, 100, 500, and 1000 h is 5.92×10^{-8}, 5.21×10^{-7}, 1.54×10^{-7}, and 1.30×10^{-7} $S\cdot cm^{-1}$, respectively. It is also worth noting that the conductivity of glasses and glass-ceramics in present work is much lower than the reported results for sealing glass-ceramics in literature.[7]

Table 1 shows the thermal properties of glasses and glass-ceramics. It is clear that the glass transition temperature (T_g) and softening temperature (T_d) increase with La_2O_3 or CeO_2 dopants. In addition, the coefficient of thermal expansion (CTE) of glasses decreases with addition of La_2O_3 or CeO_2. The increase in T_g and T_d as well as the decrease in CTE indicate the condensed glass network by La_2O_3 or CeO_2 dopants.[31] Moreover, the density of glass#GA is lower than that of glass#GL and glass#GC, which can be related to the strengthened glass structure as well as the larger atomic weight of La and Ce than other elements in the glass. The condensed glass structure contributes to the decrease in conductivity of glass (in Fig.1a), due to the enhanced restriction on the ionic diffusion.[27,30,32] On the other hand, the density of glass-ceramics after held at 750 ºC does not change significantly with heat-treatment time, which excludes the effect of glass matrix on the conductivity of glass-ceramics.[27] The CTE of glass-ceramics ranges from 9.2 to 9.7×10^{-6} K^{-1}, within the designed CTE range for sealing glass-ceramics.[22]

RSC Advances Accepted Manuscript

Fig.2a shows the XRD patterns of glass#GA held at 750 °C for up to 1000 h. The main phases in glass-ceramics are $Ca_2Al_2SiO_7$ (ICDD Card No.73-2041), $SrAl_2Si_2O_8$ (ICDD Card No.70-1862), Ca_2SiO_4 (ICDD Card No.72-1660), Sr_2SiO_4 (ICDD Card No.76-1494), and $Ca_2B_2O_5$ (ICDD Card No.79-1516). Fig.2b shows the XRD patterns of glass#GL held at 750 °C for up to 1000 h. In addition to the phases present in glass#GA, a new La-containing phase, *i.e.*, La_5SiBO_{13} (ICDD Card No.52-0699), can be observed in glass#GL. The XRD patterns in Fig.2a and Fig.2b does not change significantly with time, implying the phase stability of glass#GA and glass#GL. Based on the similar density of glass-ceramics (in Table 1) and the phase stability (in Fig.2) of glass-ceramics, one can conclude that the decrease in conductivity of glass#GA and glass#GL with increasing time is mainly attributed to the crystal growth in glass-ceramics, which reduces the number of grain boundary and consequently decreases the most effective pathway for ionic diffusion.[33,34]

Shown in Fig.2c are the XRD patterns of glass#GC held at 750 °C for up to 1000 h. It is clear that CeO_2 (ICDD Card No.81-0792) is the only phase detected in the glass-ceramic held at 750 °C for up to 100 h; whereas, some more phases can be identified from the specimen for more than 100 h, including $Ca_2Al_2SiO_7$, $SrAl_2Si_2O_8$, Ca_2SiO_4, $Ca_2B_2O_5$ and $Ca_{0.84}Sr_{1.16}SiO_4$ (ICDD Card No.77-0474). Table 2 summarizes the quantitative XRD results for glass#GC held at 750 °C for up to 1000 h. In addition, the calculated crystalline content in CeO_2-containing glass-ceramics increases from 2 wt% for 24 h to 5 wt% for 100 h. Therefore, the increase in conductivity of glass#GC from 5.92×10^{-8} $S\cdot cm^{-1}$ for 24 h to 5.21×10^{-7} $S\cdot cm^{-1}$ for 100 h relates to the increasing CeO_2 content in glass-ceramics , due to its good conductivity under SOFC operational conditions.[35] Moreover, the decrease in conductivity of glass#GC from 5.21×10^{-7} $S\cdot cm^{-1}$ for 100 h to 1.30×10^{-7} $S\cdot cm^{-1}$ for 1000 h can be

RSC Advances Accepted Manuscript

ascribed to the formation of insulative phases, such as $Ca_2Al_2SiO_7$, $SrAl_2Si_2O_8$, Ca_2SiO_4, $Ca_{0.84}Sr_{1.16}SiO_4$ and $Ca_2B_2O_5$. [36-38]

Fig.3 shows the SEM micrographs of glass#GA held at 750 °C for up to 1000 h. The gray regions are found to contain significant amount of Sr, Al and Si, confirming the formation of $SrAl_2Si_2O_8$ in glass#GA. In addition, the crystal growth can be observed by comparing the size of gray regions in Fig.3a and Fig.3b. This is in good agreement with the decrease in conductivity of glass#GA with increasing time (in Fig.1).

Fig.4 shows the SEM micrographs of glass#GL held at 750 °C for up to 1000 h. The La-enrichment can be observed in the white regions, in agreement with the formation of La_5SiBO_{13} in XRD results (in Fig.2). The crystal growth of La_5SiBO_{13} can also be observed with increasing time, which contributes to the decrease in conductivity of glass#GL with increasing time (in Fig.1).

Shown in Fig.5 are the SEM micrographs of glass#GC held at 750 °C for up to 1000 h. It is clear that some small crystalline present in glass-ceramics for 24 and 100 h (in Fig.5a and Fig.5b), which can be identified to be CeO_2. In addition, the CeO_2 crystalline scatter in glass-ceramics for 500 and 1000 h (in fig.5c and Fig.5d). This further verifies that the decrease in conductivity of glass#GC from 100 h to 1000 h results from the formation of insulative phases.

Fig.6 shows the SEM micrographs of the glass-ceramic/8YSZ sealing couples held at 750 °C for 1000 h, along with the elemental EDS line scans taken across the interface. The EDS line scans reveal the formation of an interdiffusion zone with about 4 μm thickness at the glass#GA/8YSZ interface (in Fig.6a); whereas, the thickness of the interdiffusion zone at the interface between glass#GL or glass#GC and 8YSZ is about 2 μm (in Fig.6b and Fig.6c). This indicates that the interdiffusion

RSC Advances Accepted Manuscript

between glass and 8YSZ electrolyte can be effectively reduced by addition of La_2O_3 or CeO_2. In addition, all sealing couples remain intact after holding at 750 °C for 1000 h, which can be mainly related to the close CTE between glass-ceramics and 8YSZ. The considerable amount of dendrites in glass-ceramics, *e.g.*, $SrAl_2Si_2O_8$ in all sepcies (in Figs.3-5) and La_5SiBO_{13} in glass#GL (in Fig.4), also contribute to the good sealing performance under SOFC operational conditions. [39]

4. Conclusions

The effect of La_2O_3 or CeO_2 on the phase evolution, electrical stability and chemical compatibility of sealing glass-ceramics has been investigated in this work. The addition of La_2O_3 or CeO_2 condenses the glass network and decreases the conductivity of glass. In addition, the La_2O_3-containing glass-ceramic exhibits good electrical stability under SOFC operational conditions. In contrast, the formation of CeO_2 in CeO_2-doped glass-ceramic leads to the decrease in electrical stability. Moreover, the interdiffusion between glass and 8YSZ electrolyte can be effectively reduced by addition of La_2O_3 or CeO_2. The findings on the phase evolution, electrical stability and chemical compatibility of glass-ceramics doped with rare earth oxide will shed light onto the design of stable sealing materials for SOFC applications.

Acknowledgments

The authors gratefully acknowledge the financial support of the National Natural Science Foundation of China (No. 51102045 and No. 21203202), and Program for New Century Excellent Talents in Fujian Province University (No. JA12013). They would also like to thank Zhenhuan Zheng for assistance with SEM/EDS and X-ray diffraction experiments, Fen Lin for assistance with dilatometric measurement.

RSC Advances Accepted Manuscript

References

1 N. Mahato, A. Banerjee, A. Gupta, S. Omar and K. Balani, *Prog. Mater. Sci.*, 2015, 72, 141-337.

2 K. Wang, D. Hissel, M. C. Péra, N. Steiner, D. Marra, M. Sorrentino, C. Pianese, M. Monteverde, P. Cardone and J. Saarinen, *Int. J. Hydrogen. Energ*, 2011, 36, 7212-7228.

3 X. Zhang, S. H. Chan, G. Li, H. K. Ho, J. Li and Z. Feng, *J. Power Sources*, 2010, 195, 685-702.

4 A. Choudhury, H. Chandra and A. Arora, *Renew. Sust. Energ. Rev*, 2013, 20, 430-442.

5 A. B. Stambouli; and E. Traversa, *Renew. Sust. Energ. Rev*, 2002, 6, 433-455.

6 Y. S. Chou, J. W. Stevenson, G. G. Xia and Z. G. Yang, *J. Power Sources*, 2010, 195, 5666-5673.

7 S. Ghosh, A. Das Sharma, P. Kundu, S. Mahanty and R. N. Basu, *J. Non-cryst. Solids.*, 2008, 354, 4081-4088.

8 V. Kumar, G. Kaur, K. Lu and G. Pickrell, *Int. J. Hydrogen. Energ*, 2015, 40, 1195-1202.

9 J. H. Hsu, C. W. Kim and R. K. Brow, *J. Power Sources*, 2014, 250, 236-241.

10 M. J. Pascual, A. Guillet and A. Durán, *J. Power Sources*, 2007, 169, 40-46.

11 I. W. Donald, P. M. Mallinson, B. L. Metcalfe, L. A. Gerrard and J. A. Fernie, *J. Mater. Sci.*, 2011, 46, 1975-2000.

12 M. K. Mahapatra and K. Lu, *J. Power Sources*, 2010, 195, 7129-7139.

13 M. K. Mahapatra and K. Lu, *Mater. Sci. Eng. R.*, 2010, 67, 65-85.

14 D. U. Tulyaganov, A. A. Reddy, V. V. Kharton and J. M. F. Ferreira, *J. Power Sources*, 2013, 242, 486-502.

15 S. Sakuragi, Y. Funahashi, T. Suzuki, Y. Fujishiro and M. Awano, *J. Power Sources*, 2008, 185, 1311-1314.

16 S. E. Lin, Y. R. Cheng and W. C. J. Wei, *J. Eur. Ceram. Soc.*, 2011, 31, 1975-1985.

17 Q. Zhang, Y. Zhu and Z. Li, *J. Non-cryst. Solids.*, 2012, 358, 680-686.

RSC Advances Accepted Manuscript

18 C. Ritzberger, E. Apel, V. M. Rheinberger, M. Schweiger and W. Hoeland, *PHYS CHEM GLASSES-B*, 2013, 54, 228-231.

19 A. Grandjean, M. Malki, V. Montouillout, F. Debruycker and D. Massiot, *J. Non-cryst. Solids.*, 2008, 354, 1664-1670.

20 A. Grandjean, M. Malki and C. Simonnet, *J. Non-cryst. Solids.*, 2006, 352, 2731-2736.

21 S. Huang, Q. Lu and C. Wang, *J. Alloy. Compd.*, 2011, 509, 4348-4351.

22 A. Goel, A. A. Reddy, M. J. Pascual, L. Gremillard, A. Malchere and J. M. F. Ferreira, *J. Mater. Chem.*, 2012, 22, 10042.

23 P. K. Ojha, T. K. Chongdar, N. M. Gokhale and A. R. Kulkarni, *Int. J. Hydrogen. Energ*, 2011, 36, 14996-15001.

24 A. Dutta, T. P. Sinha, P. Jena and S. Adak, *J. Non-cryst. Solids.*, 2008, 354, 3952-3957.

25 M. L. Braunger, C. A. Escanhoela Jr, I. Fier, L. Walmsley and E. C. Ziemath, *J. Non-cryst. Solids.*, 2012, 358, 2855-2861.

26 J. Chen, Q. Zou, F. Zeng, S. Wang, D. Tang, H. Yang and T. Zhang, *J. Power Sources*, 2013, 241, 578-582.

27 H. Liu, D. Zhao, S. Chen, J. Huang, D. Tang and T. Zhang, *RSC Adv.*, 2015, 5, 62891-62898.

28 S. B. Sohn and S.-Y. Choi, *J. Non-cryst. Solids.*, 2001, 282, 221-227.

29 C. H. Hsieh and H. Jain, *J. Non-cryst. Solids.*, 1995, 183, 1-11.

30 S. Chen, Z. Yu, Q. Zhang, J. Wang, T. Zhang and J. Wang, *J. Eur. Ceram. Soc.*, 2015, 35, 2427-2431.

31 Y. H. Zhang, A. Navrotsky, H. Li, L. Y. Li, L. L. Davis and S. D. M., *J. Non-cryst. Solids.*, 2001, 296, 93-101.

32 V. K. Deshpande and R. N. Taikar, *Materials Science and Engineering: B*, 2010, 172, 6-8.

33 A. C. S. Sabioni, J. N. V. Souza, V. Ji, F. Jomard, V. B. Trindade and J. F. Carneiro, *Solid State Ionics*, 2015, 276, 1-8.

34 K. Marquardt, E. Petrishcheva, E. Gardés, R. Wirth, R. Abart and W. Heinrich, *Contrib. Mineral. Petr.*, 2011, 162, 739-749.

RSC Advances Accepted Manuscript

35 M. S. H. Tinku Baidya, and J. Gopalakrishnan, *J. Phys. Chem. B*, 2007,, 111, 5149-5154.

36 H. Takeda, M. Hagiwara, H. Noguchi, T. Hoshina, T. Takahashi, N. Kodama and T. Tsurumi, *Appl. Phys. Lett.*, 2013, 102, 242907.

37 C. C. Chiang, S. F. Wang, Y. R. Wang and Y. F. Hsu, *J. Alloy. Compd.*, 2008, 461, 612-616.

38 X. C. Wang, W. Lei, R. Ang and W. Z. Lu, *Ceram. Int.*, 2013, 39, 1707-1710.

39 L. H. Fang, Q. Zhang, F. Lin, D. Tang, T. Zhang, *J. Eur. Ceram. Soc.*, 2015, 35, 2201-2207.

RSC Advances Accepted Manuscript

List of tables

Table 1 Thermal properties of glasses and glass-ceramics.

Sample ID	**glass#GA**	**glass#GL**	**glass#GC**
Thermal parameters (ºC)			
T_g	712±5	726±5	727±5
T_d	769±5	864±5	773±5
CTE (200-600 ºC)×10^{-6} (K^{-1})			
Glasses	13.3±0.1	10.7±0.1	9.9±0.1
Glass-ceramics	9.7±0.1	9.7±0.1	9.2±0.1
Density (g·cm^{-3})			
Glasses	3.24 ± 0.01	3.33 ± 0.01	3.29 ± 0.01
Glass-ceramics			
750 ºC 100 h	3.08 ± 0.01	3.28 ± 0.01	3.35 ± 0.01
750 ºC 500 h	3.18 ± 0.01	3.26 ± 0.01	3.34 ± 0.01
750 ºC 1000 h	3.11 ± 0.01	3.28 ± 0.01	3.33 ± 0.01

Table 2 Quantitative XRD results for CeO_2-containing glass-ceramics held at 750 ºC for different time (in wt%).

Time	**CeO_2**	**$Ca_{0.84}Sr_{1.16}SiO_4$**	**$Ca_2Al_2SiO_7$**	**Ca_2SiO_4**	**$SrAl_2Si_2O_8$**	**$Ca_2B_2O_5$**
24 h	100					
48 h	100					
100 h	100					
300 h	6	17	13	4	36	24
500 h	6	17	15	4	35	24
1000 h	5	17	20	6	33	19

RSC Advances Accepted Manuscript

Fig.1

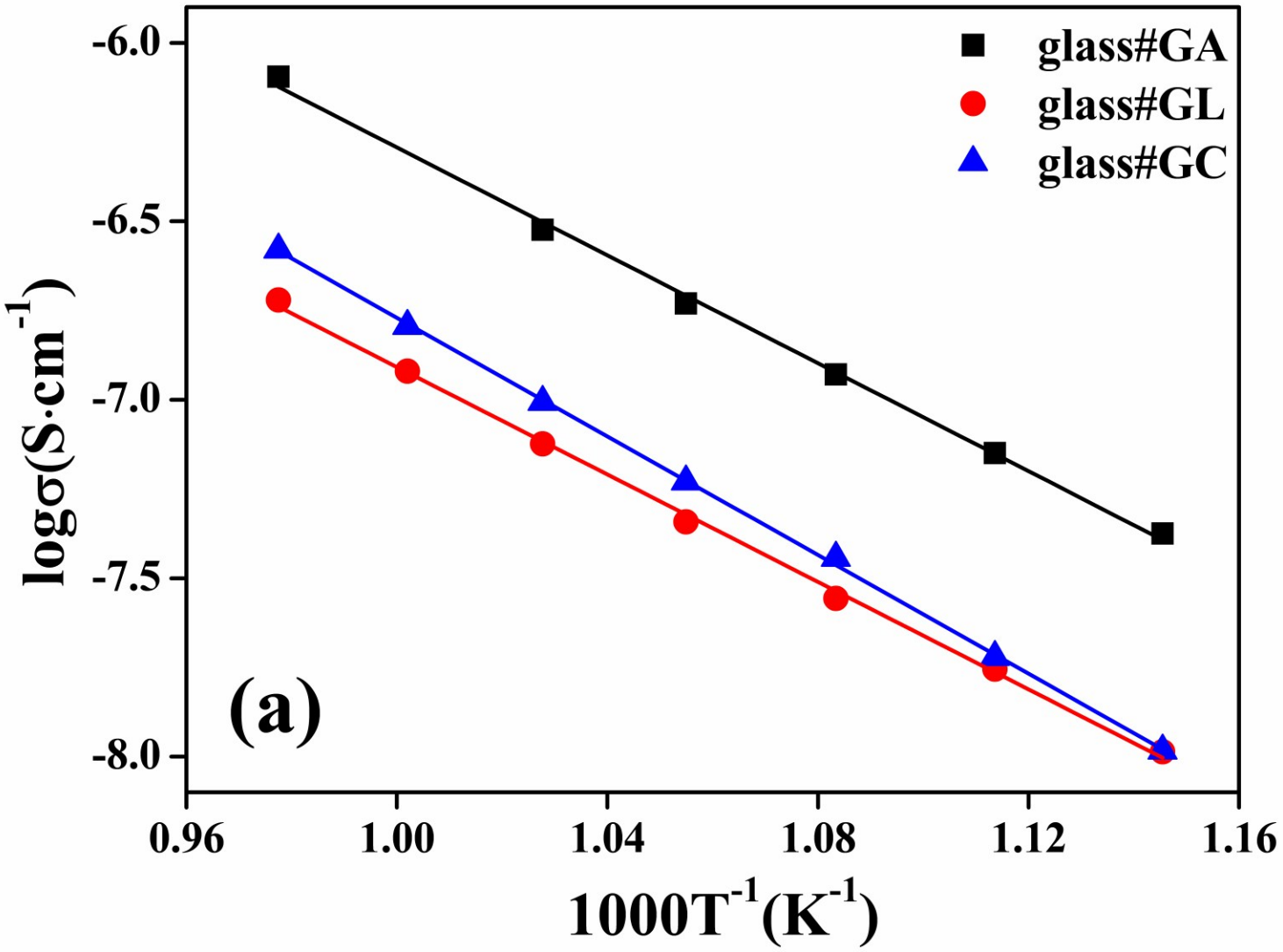

RSC Advances Accepted Manuscript

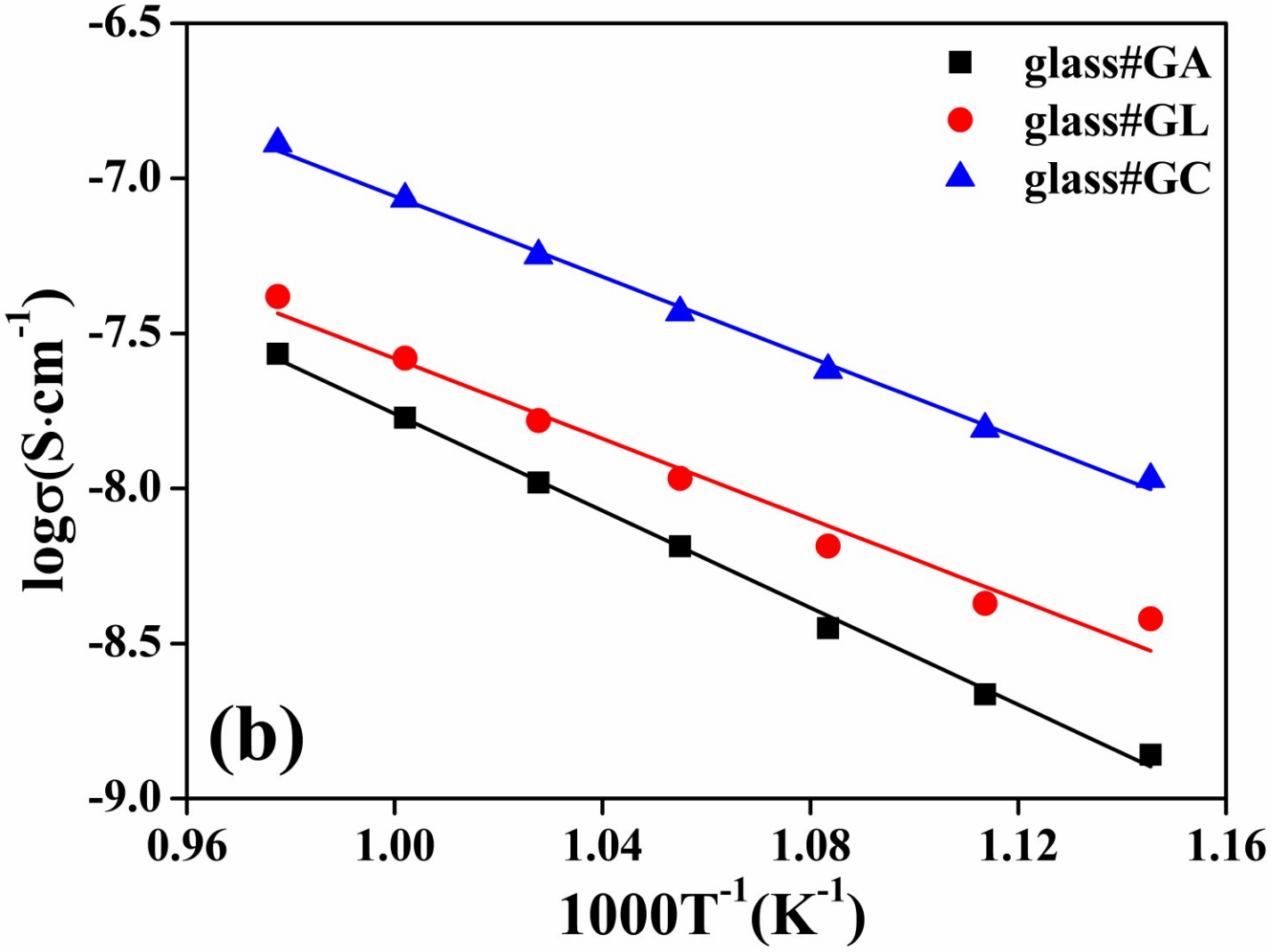

RSC Advances Accepted Manuscript

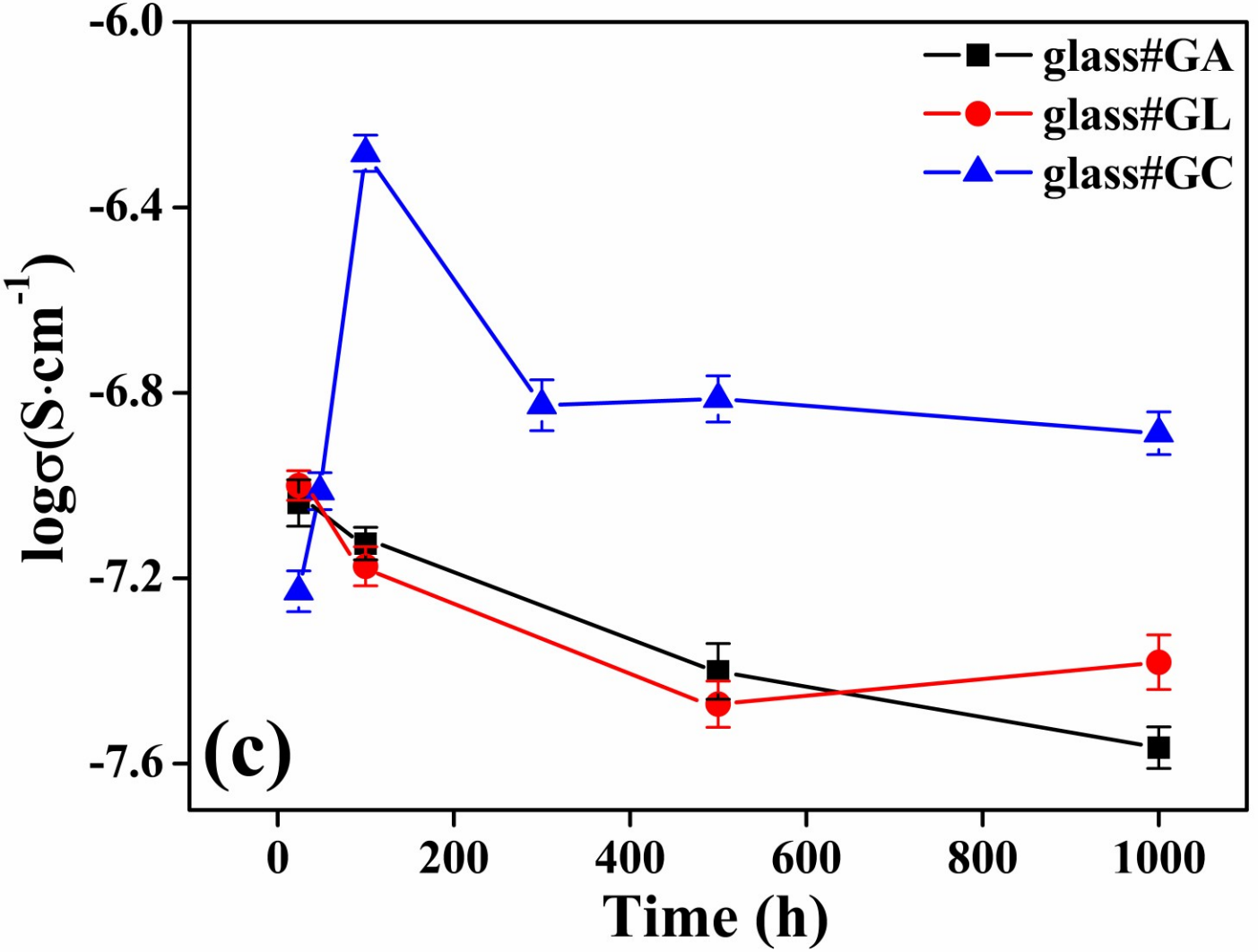

Fig.1 The temperature dependence of conductivity (log σ versus 1000 T^{-1}) for (a) glasses, and (b) glass-ceramics held at 750 ºC for 1000 h, (c) The conductivity of glass-ceramics at 750 ºC as a function of heat-treatment time.

RSC Advances Accepted Manuscript

Fig.2

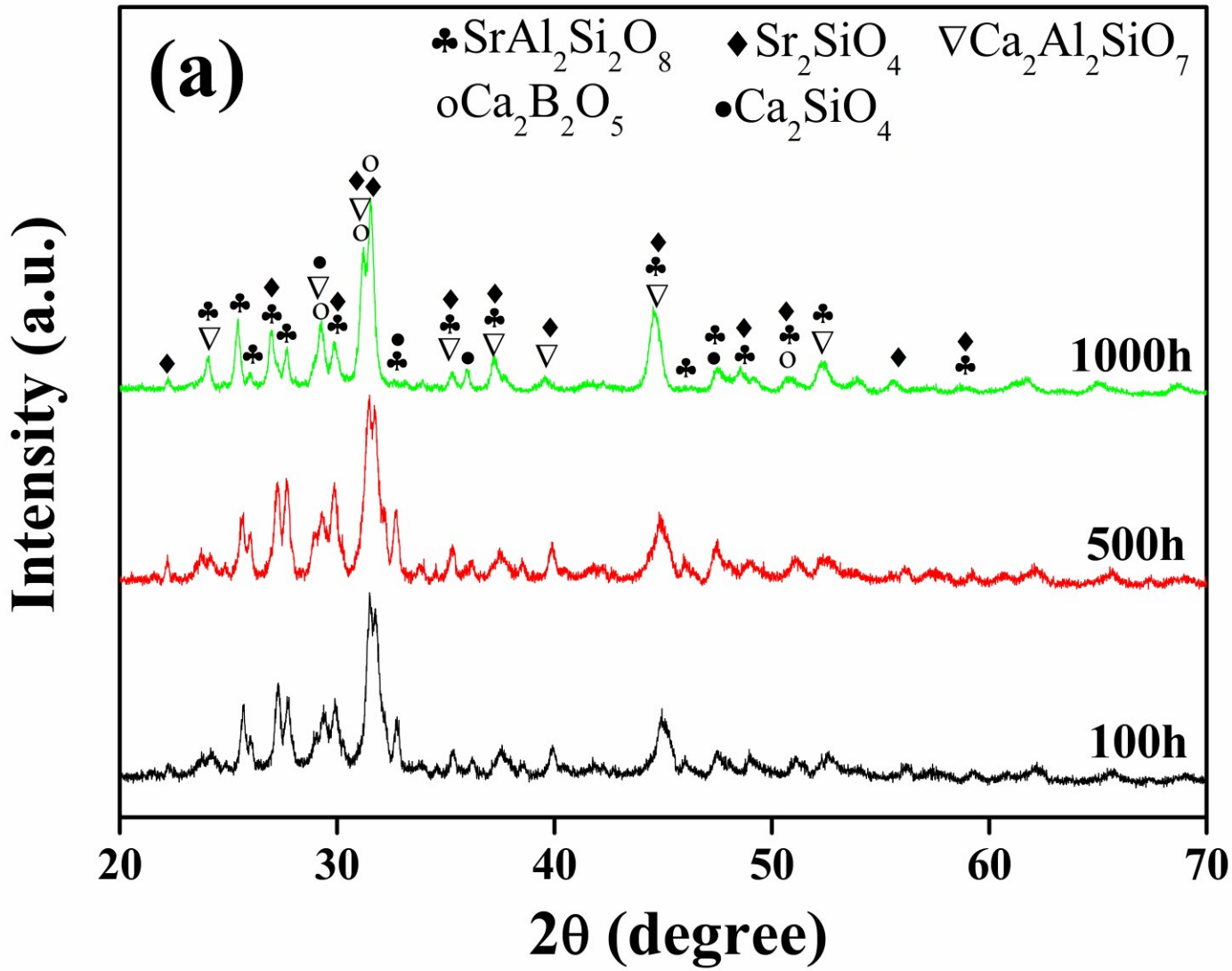

RSC Advances Accepted Manuscript

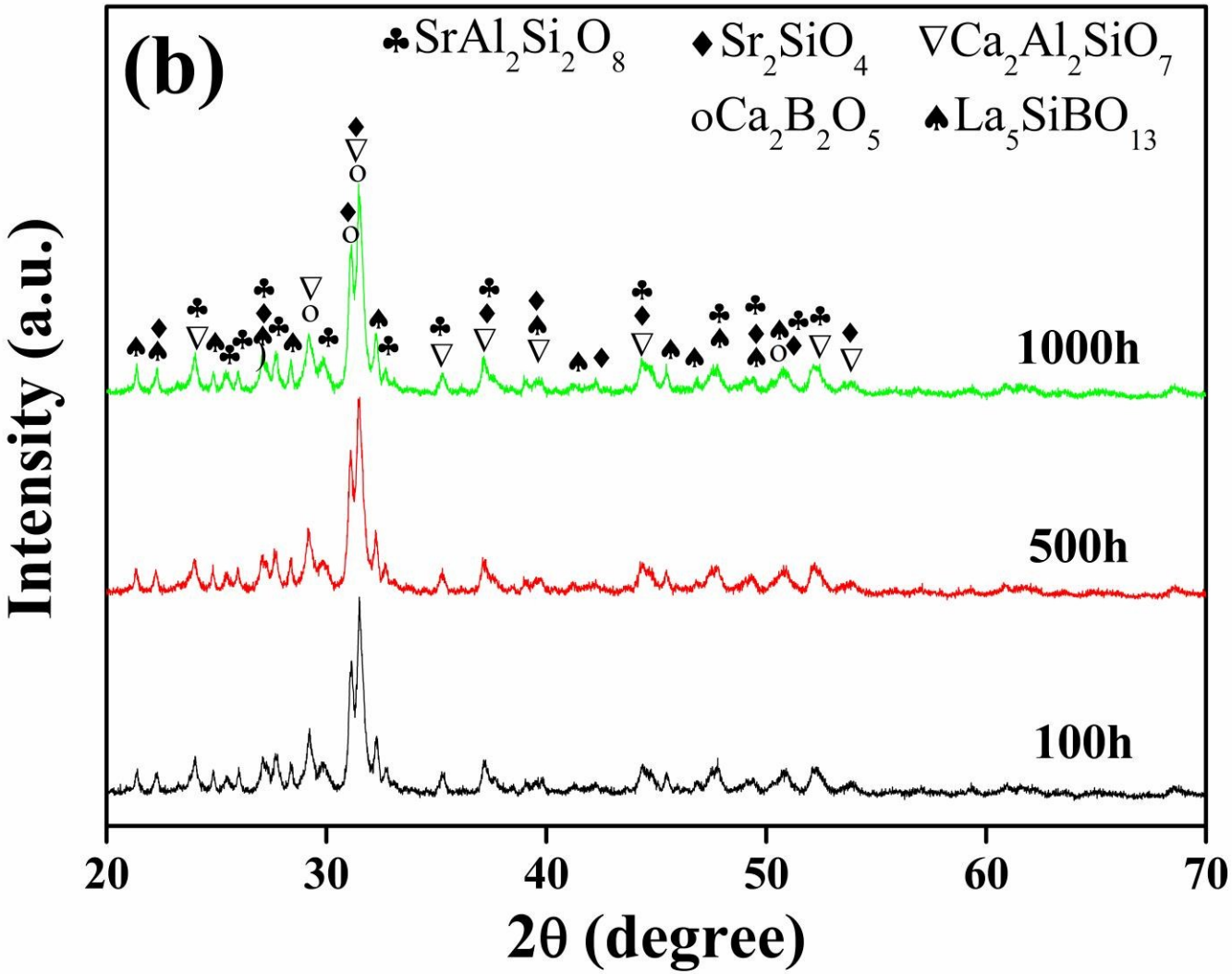

RSC Advances Accepted Manuscript

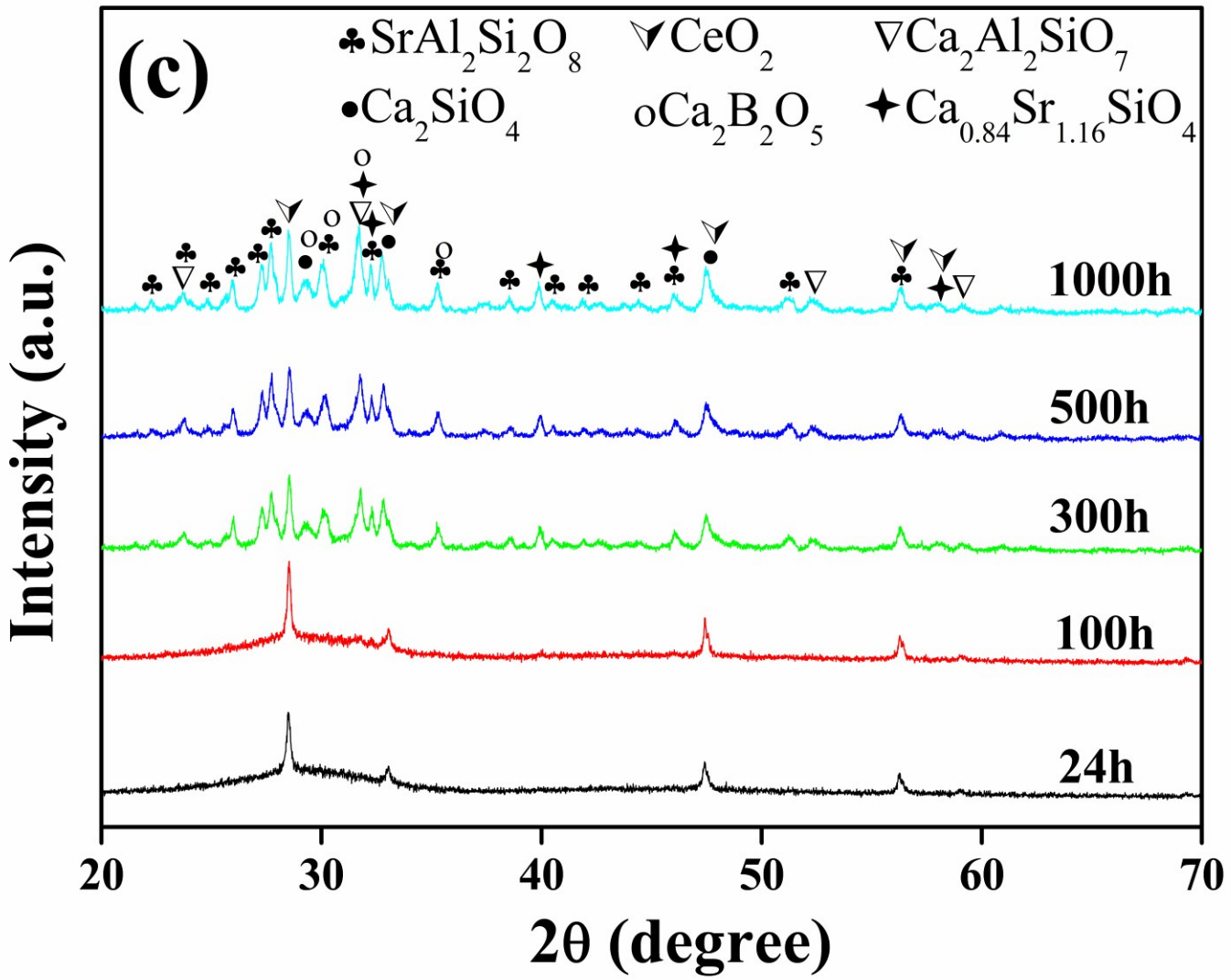

Fig.2 XRD patterns of glass-ceramics held at 750 ºC, for (a) glass#GA, (b) glass#GL, and (c) glass#GC.

RSC Advances Accepted Manuscript

Fig.3

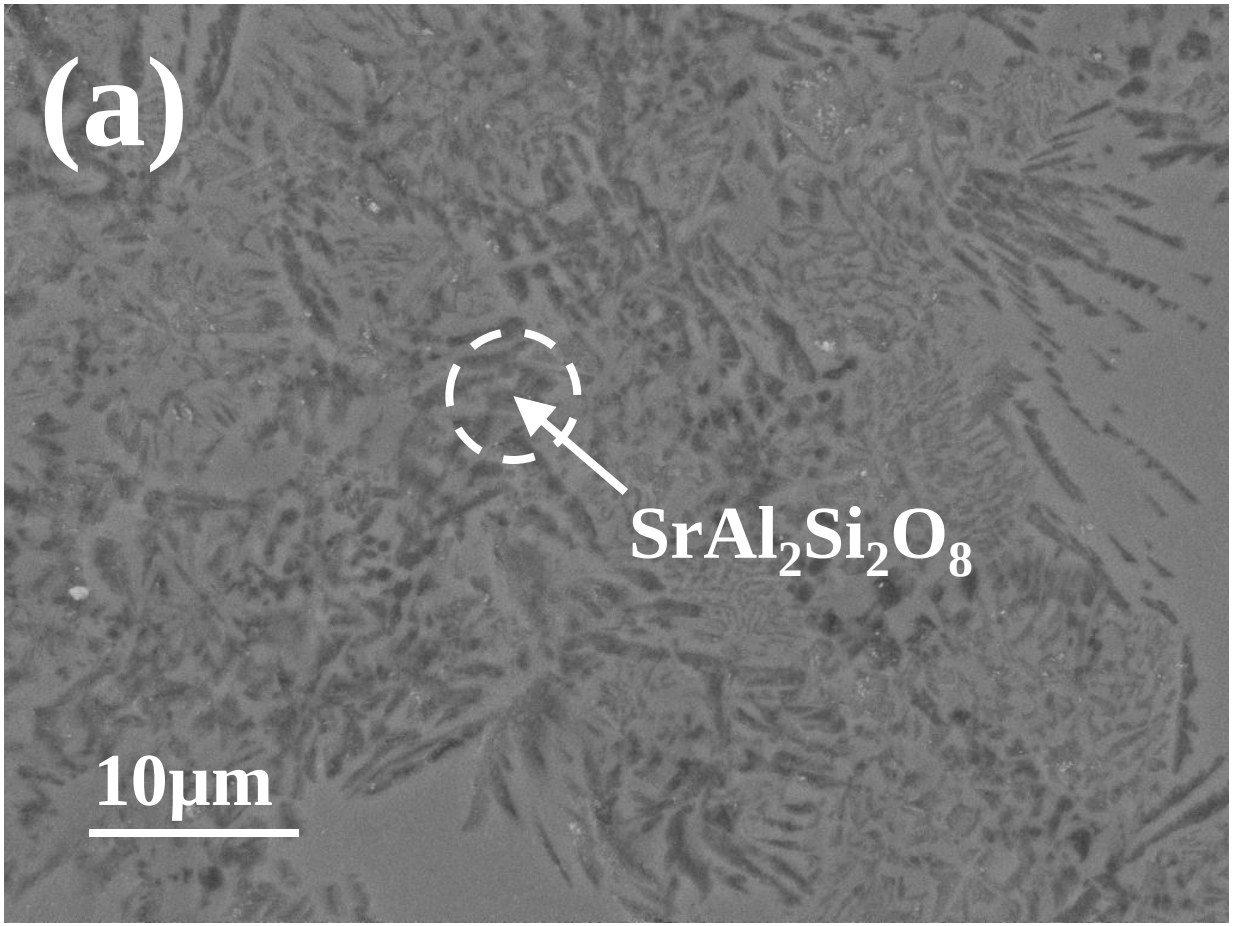

RSC Advances Accepted Manuscript

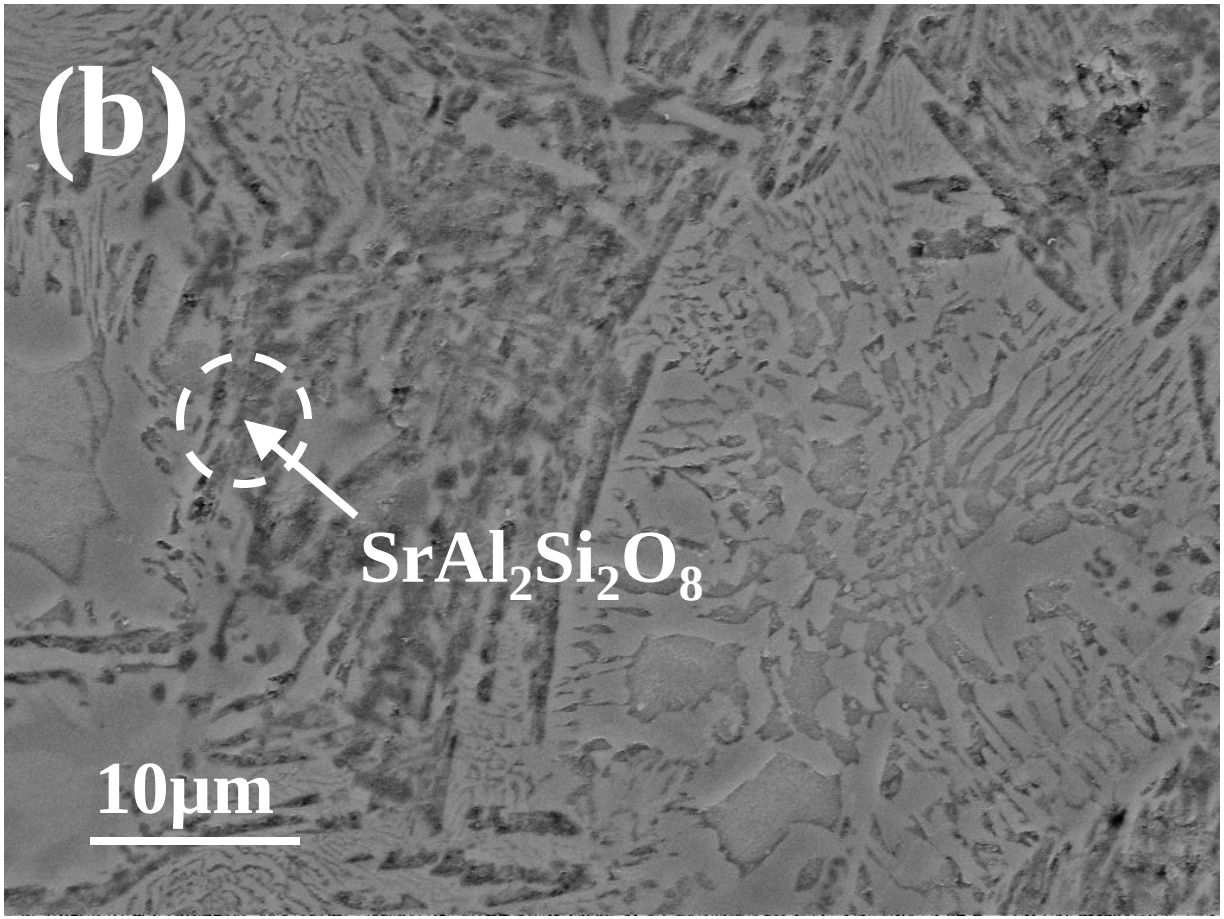

Fig.3 SEM images for glass#GA held at 750 ºC for (a) 100 h and (b) 1000 h.

RSC Advances Accepted Manuscript

Fig.4

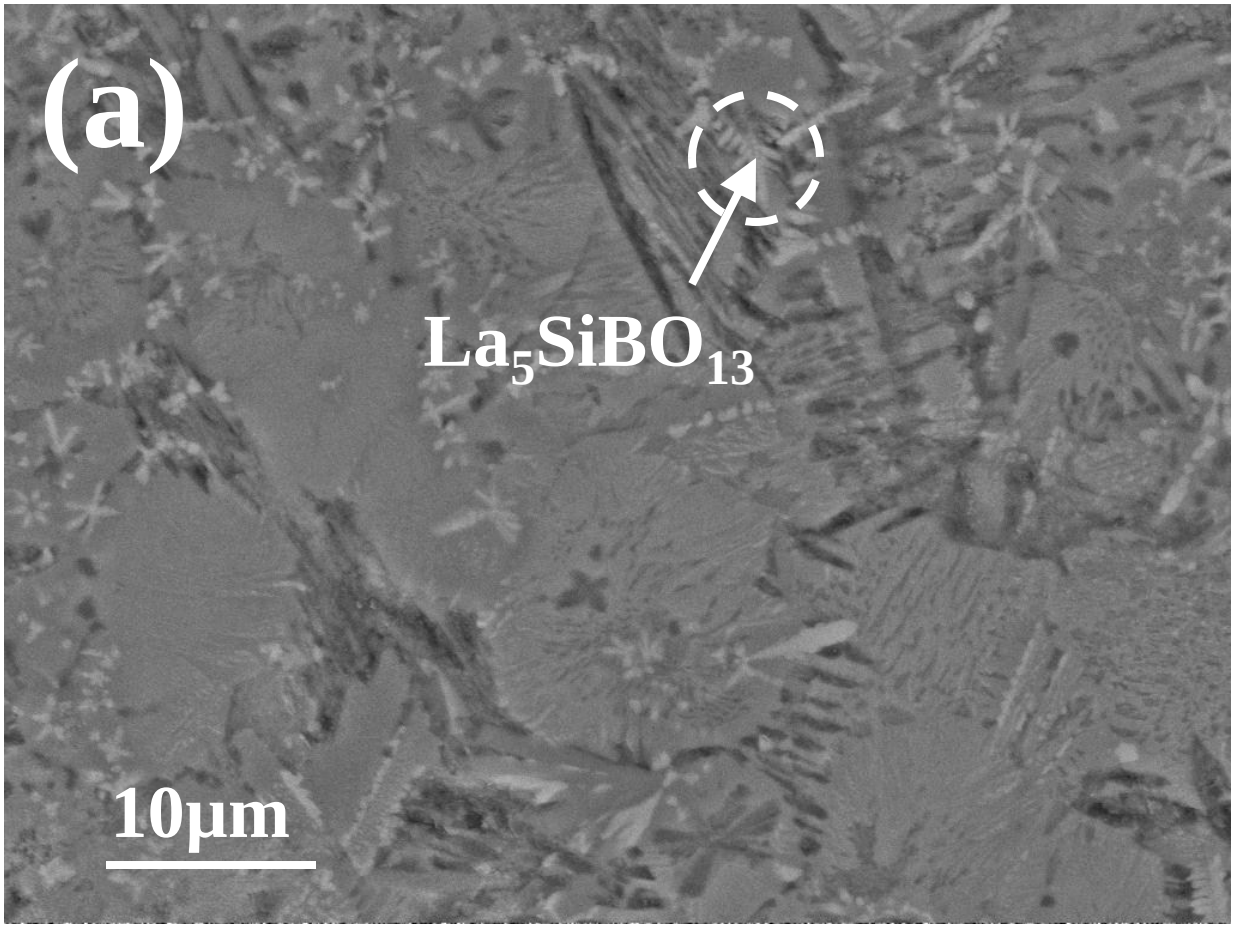

RSC Advances Accepted Manuscript

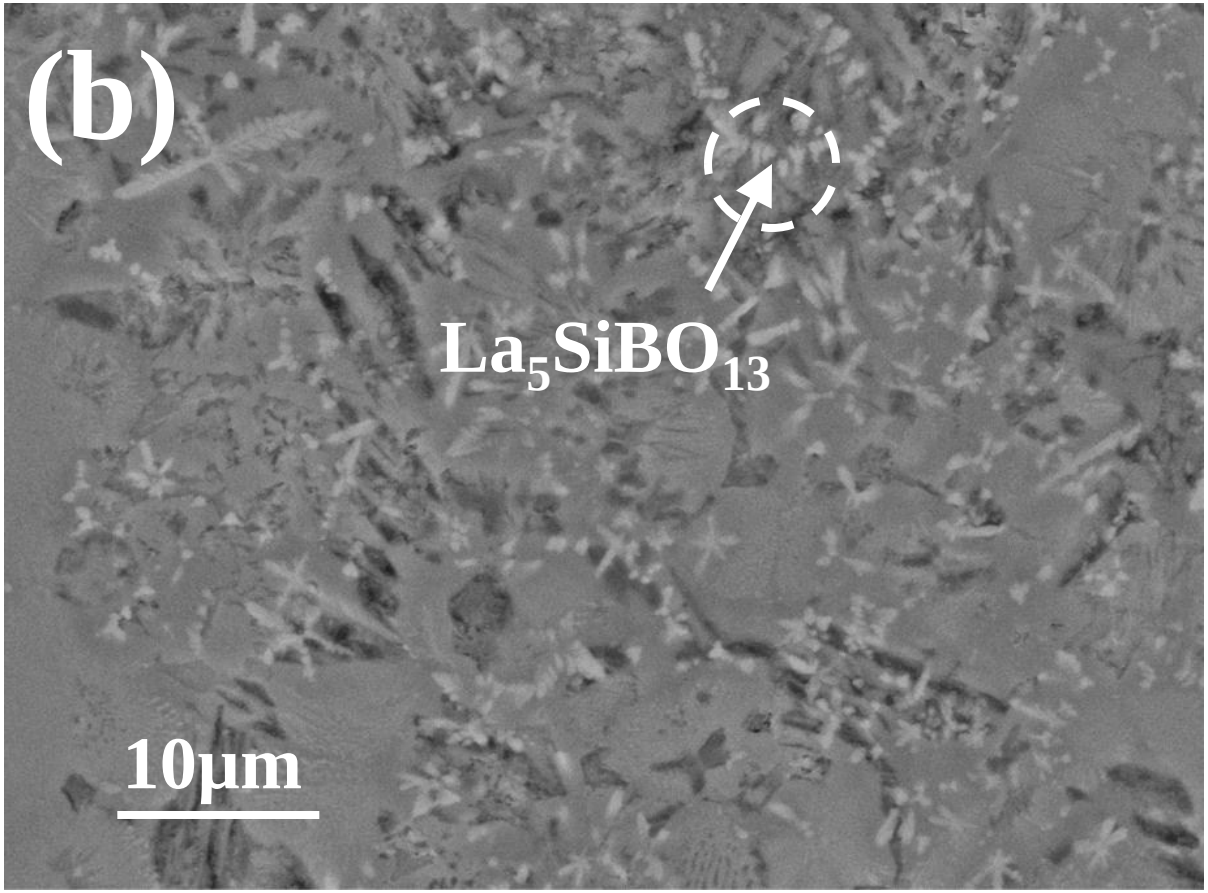

Fig.4 SEM images for glass#GL held at 750 ºC for (a) 100 h and (b) 1000 h.

RSC Advances Accepted Manuscript

Fig.5

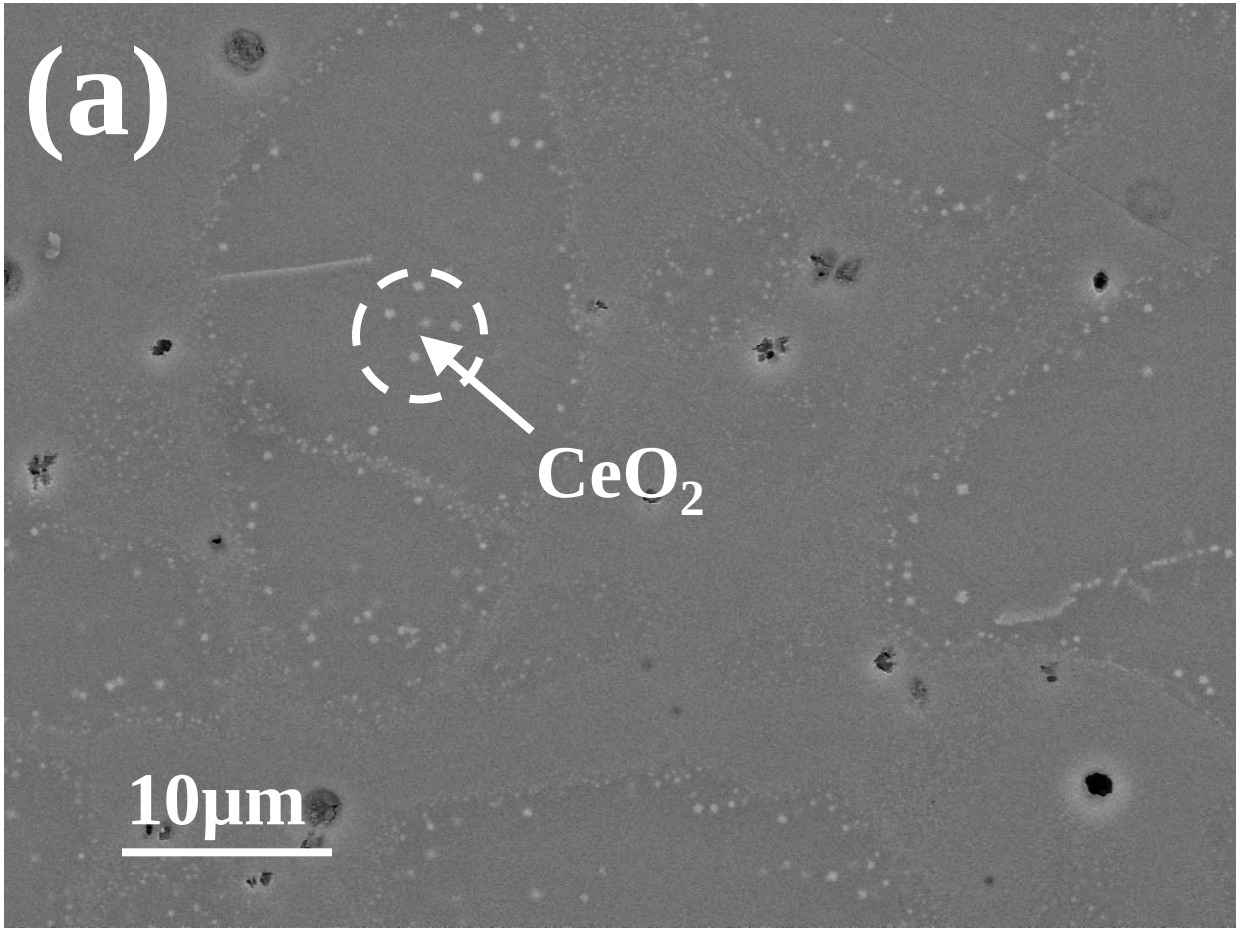

RSC Advances Accepted Manuscript

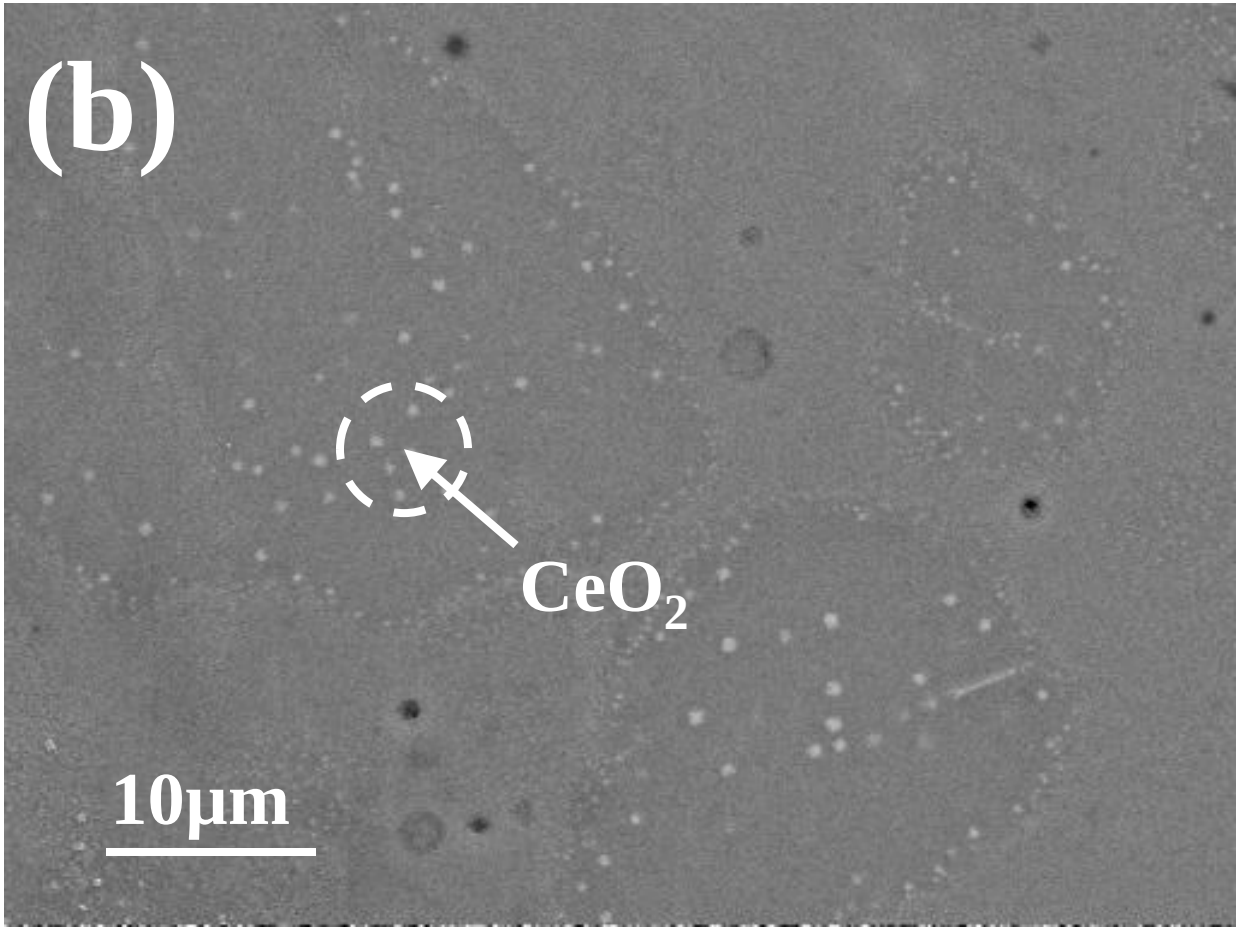

RSC Advances Accepted Manuscript

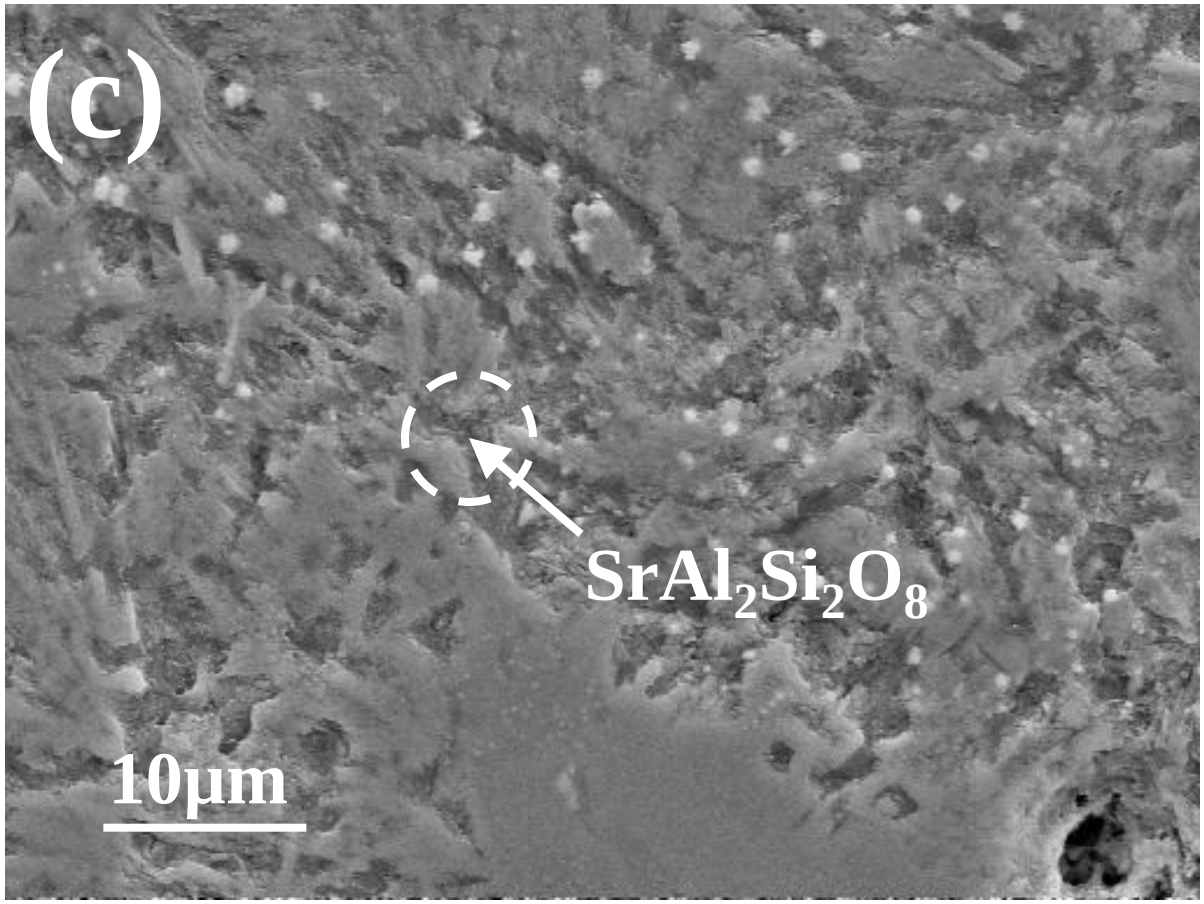

RSC Advances Accepted Manuscript

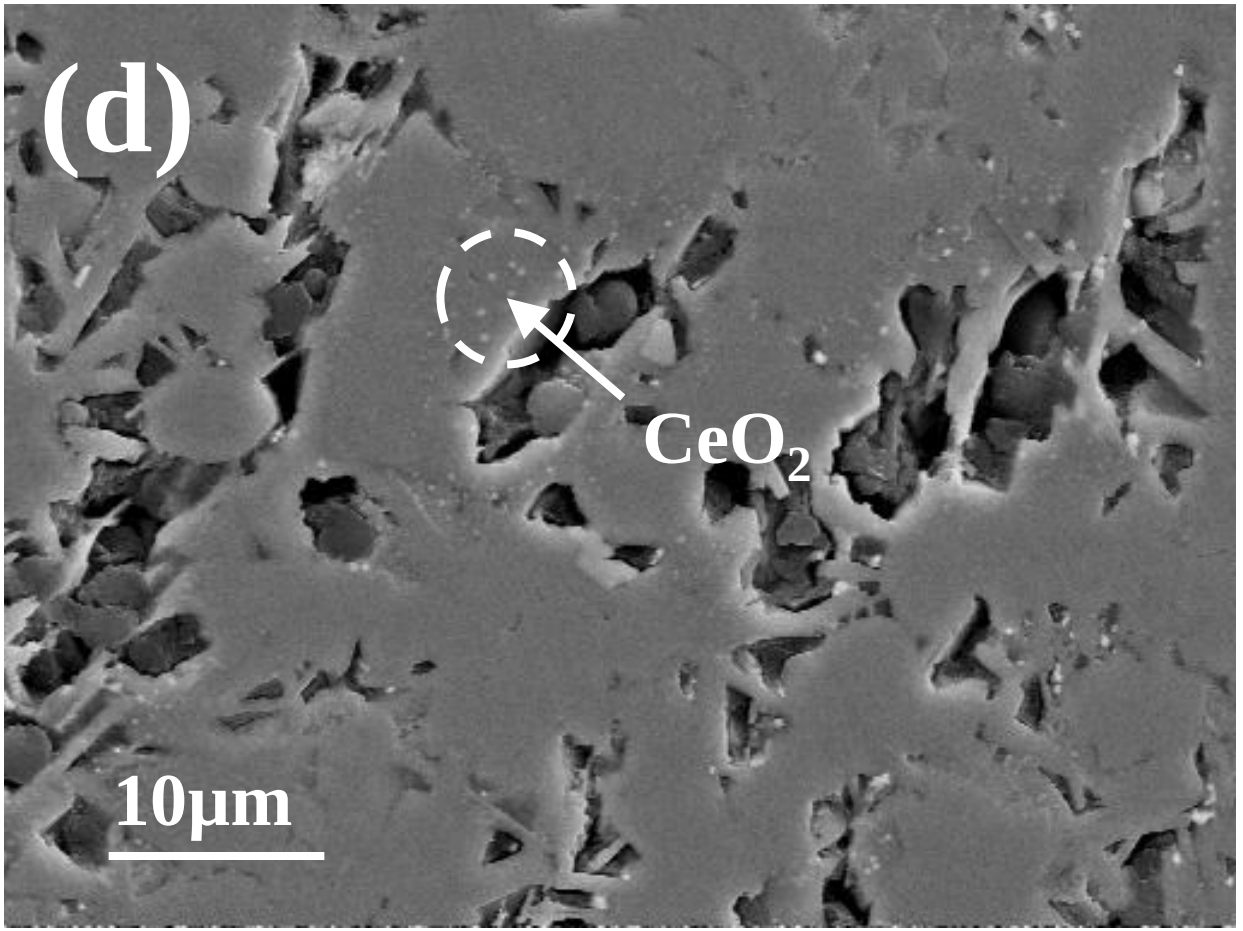

Fig.5 SEM images for glass#GC crystallized at 750 ºC for (a) 24 h, (b) 100 h, (c) 500 h, and (d) 1000 h.

RSC Advances Accepted Manuscript

Fig.6

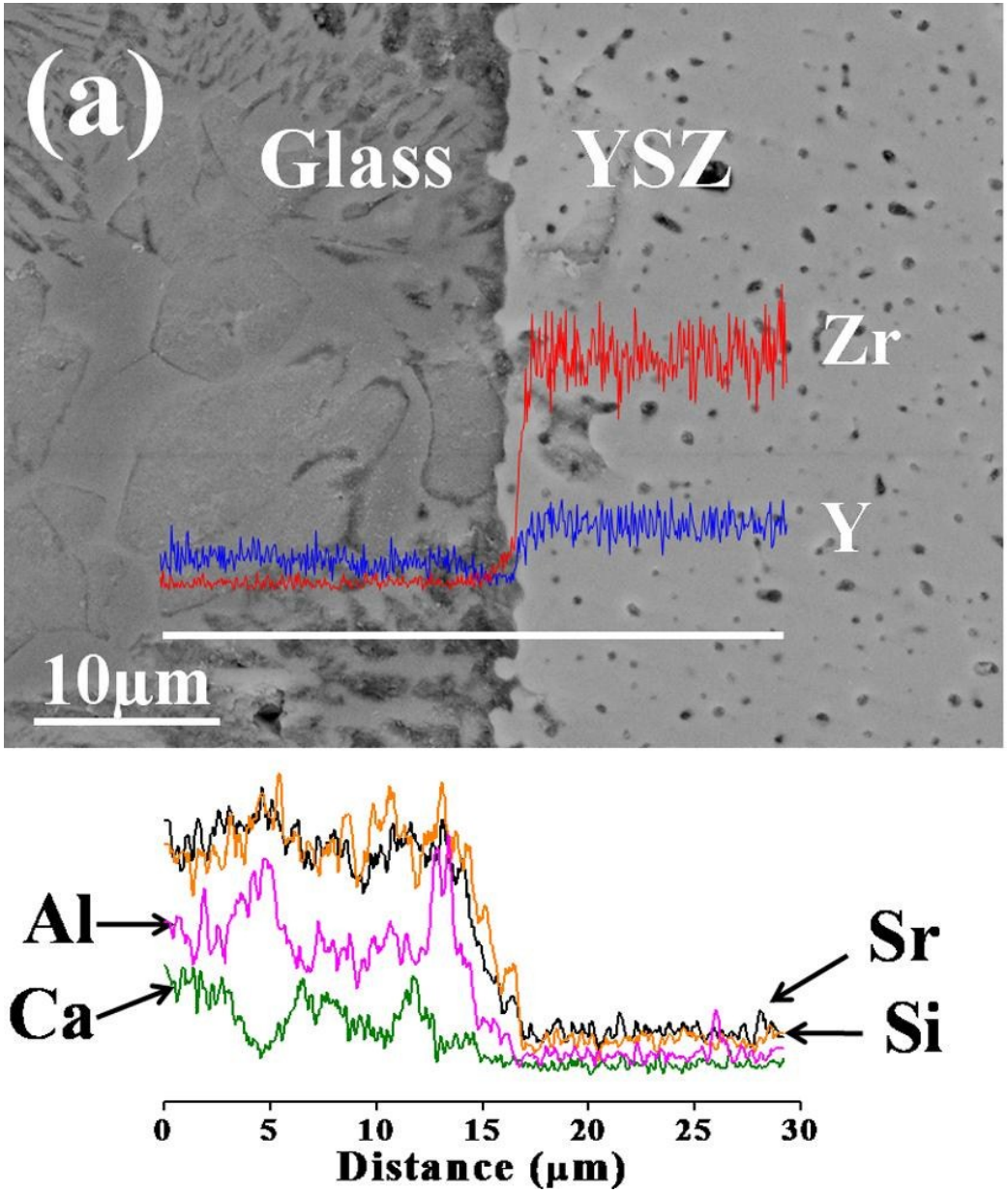

RSC Advances Accepted Manuscript

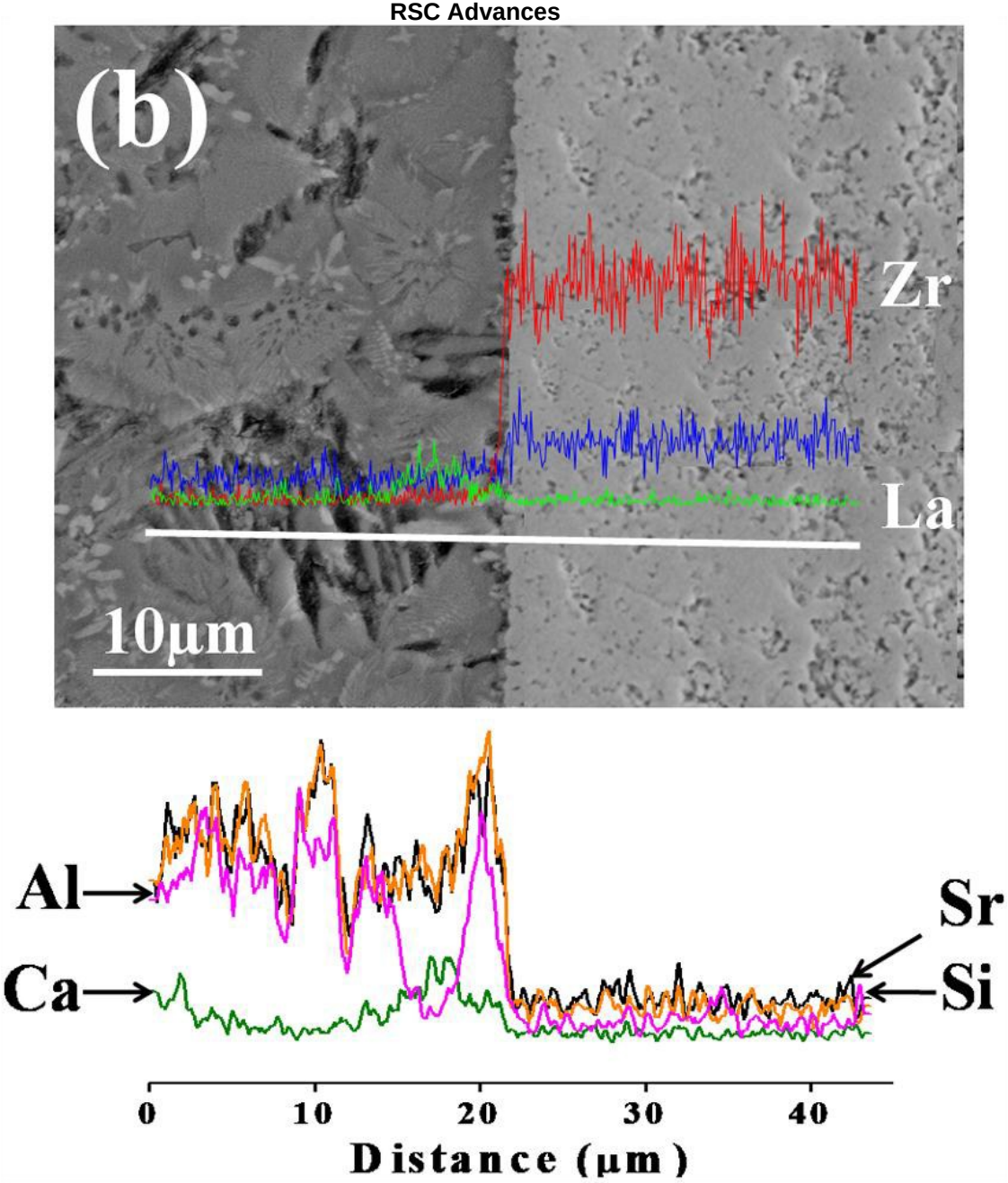

RSC Advances Accepted Manuscript

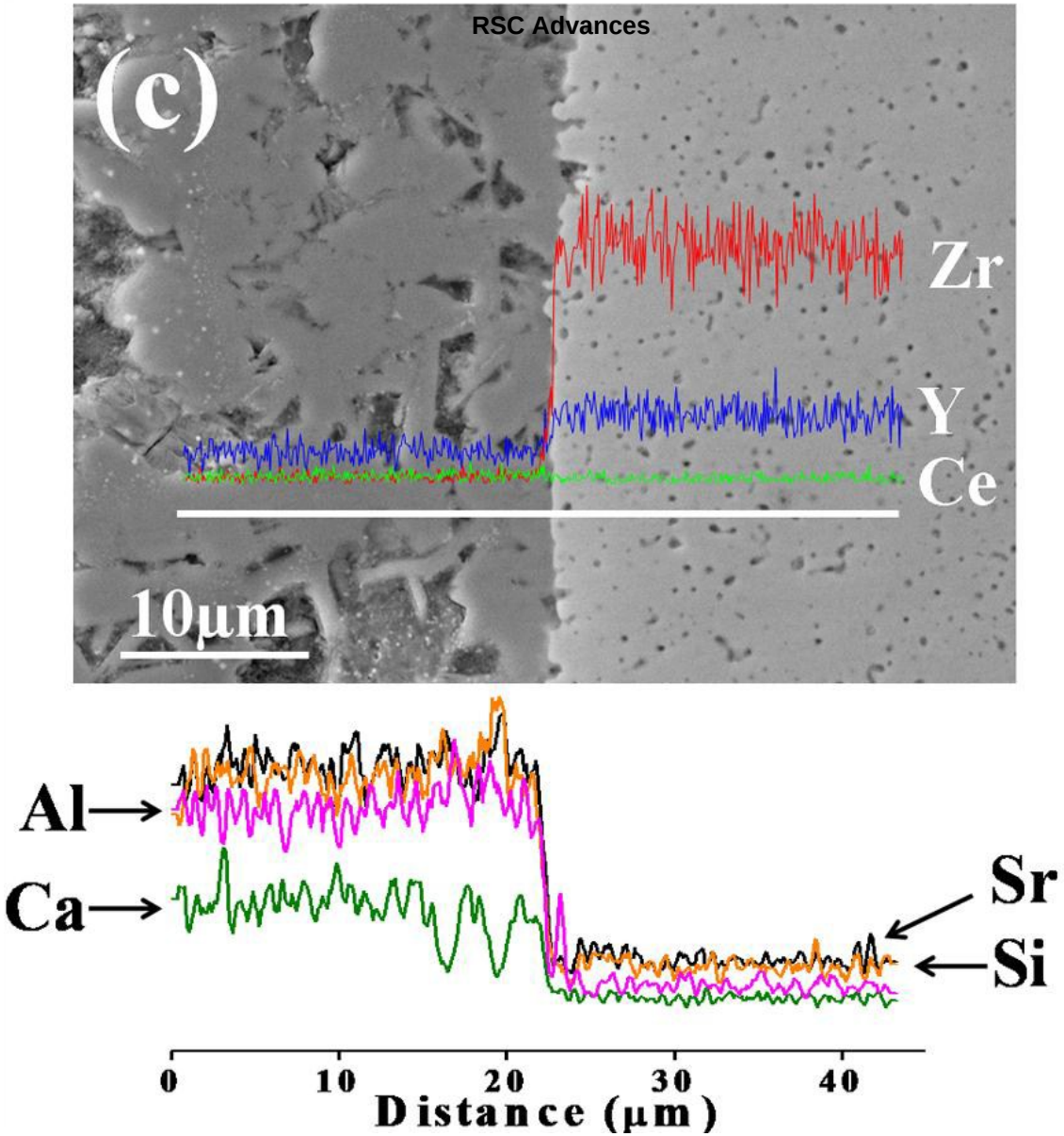

Fig.6 SEM micrographs of the glass/8YSZ sealing couples held at 750 ºC for 1000 h, along with the elemental EDS line scans taken across the interface, for (a) glass#GA, (b) glass#GL, and (c) glass#GC.

RSC Advances Accepted Manuscript

Graphical Abstract

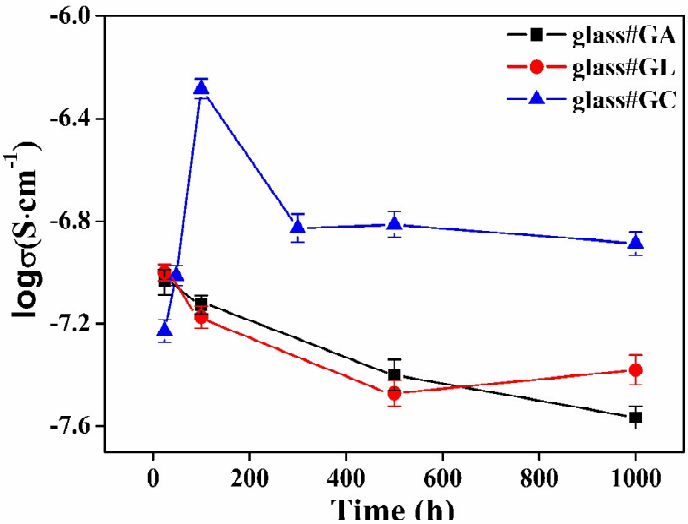

The relationship between the phase evolution and the change in conductivity of glass-ceramics has been clearly demonstrated in this work.

RSC Advances Accepted Manuscript